International Journal of Engineering Research for Sustainable Development

Peer Reviewed International, Open Access Journal.

ISSN : 3067-2325 / Website: https://ijersd.com / Volume 2 /Issue 1 / February 2026

Original Article

Study of the Electrochemical performance of perovskite LaMnO3

Tanay S. Gore

Dnyanopasak Shikshan Mandal's Arts, Commerce and Science College, Parbhani, India

School of Physical Sciences, SRTM University, Nanded, India

Manuscript ID: IJERSD-2026-020106

ISSN: 3067-2325

Volume 2

Issue 1

Pp 26-30

February 2026

Submitted: 05 Jan. 2026

Revised: 15 Jan. 2026

Accepted: 10 Feb 2026

Published: 28 Feb 2026

Correspondence Address:
Tanay S. Gore
Dnyanopasak Shikshan Mandal's Arts, Commerce and Science College, Parbhani, India
School of Physical Sciences, SRTM University, Nanded, India
Email: goretanay@gmail.com

Quick Response Code:

Web. https://rlgjaar.com

DOI: 10.5281/zenodo.21944230

DOI Link:
https://doi.org/10.5281/zenodo.21944230

Abstract

$LaMnO_3$ soft ferrite nanoparticles were successfully synthesized using the citrate–nitrate auto-combustion method and investigated as electrode materials for electric double-layer capacitor (EDLC)-type supercapacitors. The LaMnO3 sample was prepared on nickel foam using the hydrothermal method. The prepared sample was calcined in air at 500°C for 2 h. The prepared sample is subjected to electrochemical performance cyclic voltammetry (CV). The charge-discharge process of the sample is determined using galvanostatic charge-discharge (GCD), and its impedance is calculated using electrochemical impedance spectroscopy (EIS). The Na2ClO4 is used as an electrolyte for the electrochemical measurement. The specific capacitance of the sample changed from 214 F g-1 to 75 F g-1 when the current density increased from 1 to 8 A g-1.

Keywords: *$LaMnO_3$; Perovskite oxide; Supercapacitor; Electric double-layer capacitor (EDLC); Electrochemical impedance spectroscopy (EIS); Cyclic voltammetry (CV); Galvanostatic charge–discharge (GCD); Energy storage.*

Introduction

Metal oxide materials are the best choice for supercapacitors, offering high-rate performance, energy-storage characteristics, and excellent cycle retention required for energy storage devices. [1]. By combining various metal oxides, it is possible to improve electrical conductivity, electrochemical performance, and cycling duration [2]. Previous studies have shown that the best supercapacitor electrode materials are metal oxides, for example, Mn-Ni, Co-Ni, and Mn-Co. Among transition metals, Mn is a promising material with excellent performance and can serve as an electrode for a supercapacitor due to its good long-term stability, redox activity, and high reversibility. Mn is abundant; therefore, we have chosen Mn2+ for supercapacitor studies [3-5].

Perovskites are inorganic materials with the general formula ABX3 [6]. The perovskite material has attracted researchers from various disciplines, including materials science, chemistry, and physics, for its diverse properties [7]. LaMnO3 has a perovskite structure and exhibits interesting chemical and physical properties useful for electrochemical reactions [8]. When the A and B ions in the perovskite structure vary, the structure remains stable; therefore, we can improve its physical and chemical properties by changing the A and B elements. In ABO3, the A-site cation is a trivalent lanthanide (Sm3+, Bi3+, La3+, etc.) or a bivalent alkali-earth element (Ba2+, Sr2+, etc.), and the B site is occupied by transition elements (Mn, Co, Ni, Fe, etc.).
In this work, we prepared a LaMnO3 sample through the hydrothermal method. The electrochemical performance has been investigated, and its influence assessed.

Synthesis and Characterization of $LaMnO_3$ system

In the present work, a LaMnO3 perovskite sample was prepared by the hydrothermal method. The high-purity AR-grade (99.99%) starting materials used were La (NO3) 3 · 6H2O, manganous nitrate (Mn (NO3)2 · 5H2O), (99.9% sd-fine). All reagents were weighed in stoichiometric proportions. All the metal nitrates were dissolved in a specified amount of deionized water and mixed together to obtain a clear solution. The reaction was carried out in a natural medium. The autoclave was heated at 100°C for 8 h. The as-prepared sample was heated at 500°C for 2 h to get the final product. The heat-treated sample was used for further characterization.

LaMnO3, as the active electrode material, and its performance in an ELDC-type supercapacitor were examined using cyclic voltammetry (CV), galvanostatic charge-discharge rate measurements, and electrochemical impedance spectroscopy (EIS). The LaMnO3-based electrode on nickel foam, with an area of 1 cm^2, was used for all the above performances.

How to cite this article:
Gore, T. S. (2026). Study of the Electrochemical performance of perovskite LaMnO3. International Journal of Engineering Research for Sustainable Development, 2(1), 26–30. https://doi.org/10.5281/zenodo.21944230

Result and discussion

Cyclic Voltammetry and Galvanostatic Charge-Discharge Tests

To investigate the charge-storage characteristics of the $LaMnO_3$-coated nickel foam electrode, cyclic voltammetry (CV) and galvanostatic charge–discharge (GCD) techniques were employed. The CV curves were recorded over a potential range of 0.2–0.7 V at scan rates of 5- 100 mV s^{-1}, as shown in Fig. 1.

Table.1. Electrochemical specification

Scan rate (A/g)	Discharge time (s)	Specific capacitance (F/g)
1	136	214.1732283
2	65	204.7244094
3	34	160.6299213
4	23	144.8818898
5	16	125.984252
8	6	75.59055118
Deposited mass	1.27 mg	
Potential window	0.5 V	
Charge transfer ratio (R_{ct})	17.08 ohm	Calculated using EIS (half circle)

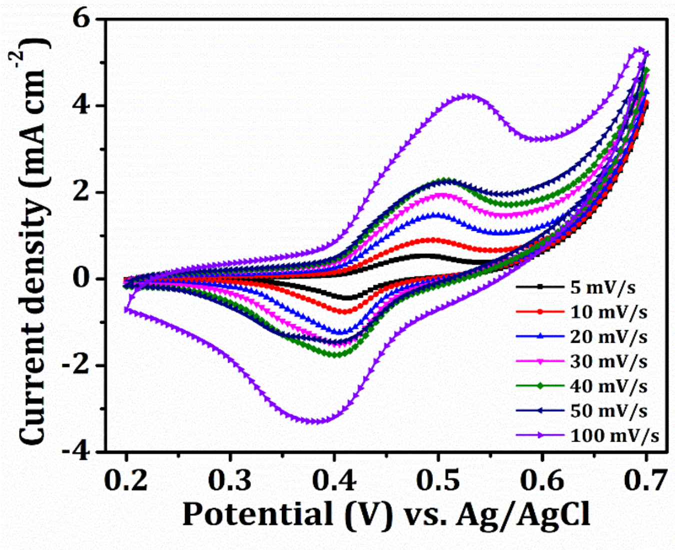

Figure 1. CV profiles of the $LaMnO_3$-based electrode with scan rates of from 5 to 100 mV s^{-1} for a supercapacitor device

In this potential window, the lowest scan rate of 5 mV s^{-1} was maintained, and the performance at this rate shows a nearly rectangular shape, indicating a predominantly non-Faradaic charge-storage mechanism. Faradaic redox peaks showing electric double-layer capacitance (EDLC)-type behavior were investigated. Increased internal resistance and polarization effects during the ultrafast charging–discharging process indicate that the slight asymmetry observed in the CV curves at higher scan rates can be attributed to these effects. Such non-Faradaic behavior is characteristic of electric double-layer capacitors, whereas pseudocapacitors or supercapacitors primarily store charge through reversible Faradaic redox reactions. The areal and specific capacitances of the fabricated supercapacitor device were calculated from the CV curves using the following equations:

$$C_{areal} = F/cm^2 = \frac{\int \Delta V \, i \, dV}{\Delta V \times S \times A} \quad (1)$$

$$C_{specific} = F/g = \frac{\int \Delta V \, i \, dV}{\Delta V \times S \times m} \quad (2)$$

where the potential window corresponding to the cathodic current is represented by ΔV , s is the scan rate (V s^{-1}), A is the area of the two electrodes (cm^2), and m is the active mass of the material deposited on both electrodes (g). The areal and specific capacitances of the fabricated device, calculated from the CV curves, varied from 214 F g^{-1} to 75 F g^{-1} as the scan rate increased. The typical characteristic of electric double-layer capacitors (EDLCs) observed decrease in capacitance with increasing scan rate is a, arising from limitations in ion diffusion and charge transport kinetics at higher scan rates. In the porous structure of the $LaMnO_3$ active layer, electrolyte ions penetrate deeply and have sufficient time to do so, resulting in enhanced charge accumulation and higher capacitance at lower scan rates. In contrast, ion diffusion becomes restricted, and charge storage predominantly occurs at the electrode's outer surface, leading to a reduction in capacitance at higher scan rates.

Figure 2 presents the galvanostatic charge–discharge (GCD) profiles recorded within a potential range of 0.0–0.5 V. The charge–discharge curves exhibit a nearly symmetrical shape, and the discharge segments remain highly linear following the initial iR drop, even at low current densities. These features are characteristic of predominantly non-Faradaic electric double-layer capacitance (EDLC) behavior in the $LaMnO_3$-based supercapacitor. The IR drop at the beginning of the discharge cycle is attributed to the internal resistance at the electrode-electrolyte-current collector interfaces. Furthermore, the pronounced linearity and symmetry of the GCD curves suggest efficient ion transport, excellent charge–discharge reversibility, and stable capacitive performance. The areal and specific capacitances were determined from the discharge curves' linear portion using the following equations:

$$C_{areal} = F/cm^2 = \frac{i}{\frac{dV}{dt} \times A} \quad (3)$$

$$C_{specific} = F/g = \frac{i}{\frac{dV}{dt} \times m} \quad 4$$

where i represents the constant applied current (A), dV/dt is the discharge curve slope measured within the potential range of 0.0–0.5 V for consistency, while m and A retain their previously defined meanings as the active mass of the material and the average area of the electrodes, respectively. The areal and specific capacitances calculated from galvanostatic charge–discharge (GCD) curves varied from 214 F g^{-1} to 75 F g^{-1} as the current density increased from 1 A g^{-1} to 8 A g^{-1}. The gradual decrease in capacitance at higher current densities is attributed to insufficient time for electrolyte ions to fully diffuse into the porous electrode structure during rapid charge–discharge cycles. Consequently, charge storage becomes increasingly surface-limited at higher current densities, resulting in reduced capacitance. The energy and power densities calculated from cyclic voltammetry (CV) and galvanostatic charge–discharge measurements are summarized in Table .1. The results demonstrate the promising electrochemical performance of the fabricated $LaMnO_3$ supercapacitor device. Furthermore, the device's energy density could be enhanced by extending the operational potential window, provided that the electrolyte and electrode materials remain electrochemically stable within the expanded voltage range.

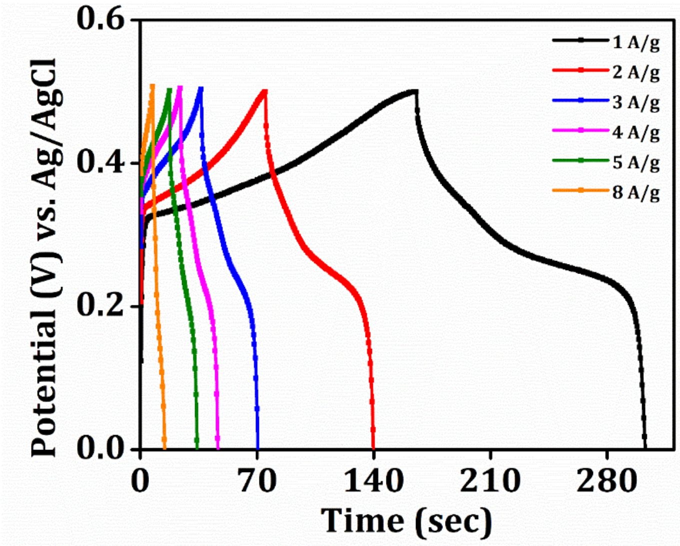

Figure 2 Galvanostatic charge−discharge curves of the $LaMnO_3$ −based EDLC under varying current density.

Cyclic stability test

The stability of the $LaMnO_3$ electrodes was examined at a 2 A g^{-1} current density over 500 consecutive galvanostatic charge–discharge cycles (GCD). The $LaMnO_3$ supercapacitor retained 99.7% of its initial capacitance even after prolonged cycling, demonstrating the excellent electrochemical stability, reversibility, and structural robustness of the $LaMnO_3$ electrodes under continuous charge–discharge operation. The outstanding capacitance retention indicates minimal degradation of the electrode material and confirms its suitability for long-term energy storage applications.

Electrochemical Impedance Spectroscopy

The impedance (resistive and capacitive) characteristics of the $LaMnO_3$-based supercapacitor were examined using electrochemical impedance spectroscopy (EIS) measurements to better understand ion diffusion and charge transport within the device. The EIS analysis was performed using an AC perturbation amplitude of 10 mV over a frequency range from 150 kHz to 0.1 Hz, with the baseline potential maintained at 0 V. Figure 3 presents the Nyquist plot of the $LaMnO_3$ supercapacitor prior to the 5000 galvanostatic charge–discharge cycles, where the imaginary (out-of-phase) impedance component is plotted against the real (in-phase) impedance component. The Nyquist plot in the high-frequency domain is represented by a semicircle, and the low-frequency region by a nearly vertical line, corresponding to charge-transfer resistance and ideal capacitive behavior, respectively. To further analyze the device's electrochemical response, the Nyquist, Bode, and frequency–phase angle plots were fitted using a modified Randles equivalent circuit model. An equivalent circuit was employed to evaluate key electrochemical parameters, including solution resistance, charge-transfer resistance, double-layer capacitance, and ion-diffusion characteristics at the electrode/electrolyte interface. The fitting results confirm the efficient charge transport properties and favorable capacitive behavior of the fabricated $LaMnO_3$ supercapacitor device.

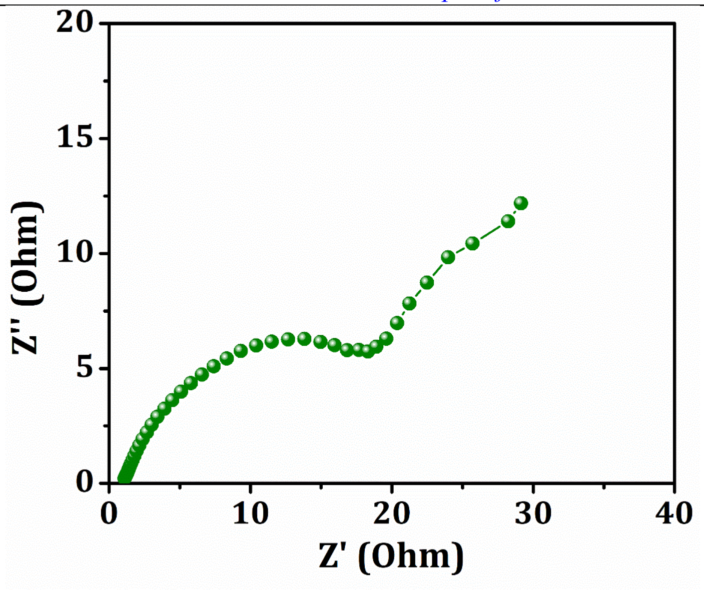

Figure 3 Nyquist plots.

The impedance spectrum of a typical electric double-layer capacitor (EDLC) is characterized by a semicircle at high frequencies and a straight line in the low-frequency domain. The intercept of the high-frequency end of the semicircle with the real impedance (Z′) axis corresponds to the value of R1 in the equivalent circuit. This parameter represents the combined resistance of the aqueous $NaClO_4$ electrolyte, intrinsic electrode resistance, and current-collector resistance, collectively referred to as the equivalent series resistance (ESR). Since charge migration and ion transport during the charge–discharge process occur through the electrolyte, R1 is connected in series with the remaining circuit elements. The fitted ESR value was 17 Ω, as shown in Table 1, indicating relatively low internal resistance and favorable electrical conductivity in the supercapacitor device. The diameter and curvature of the semicircular region were simulated using a constant phase element (Q1) and a resistor (R2) connected in parallel, which represent interfacial charge-transfer processes and non-ideal capacitive behavior at the electrode/electrolyte interface. In the high-frequency region, the short charging duration prevents electrolyte ions from diffusing effectively into the inner pores of the $LaMnO_3$ electrode material. Instead, the ions accumulate mainly at the electrode surface, forming an electrostatic double layer that accounts for the observed capacitive response.

Conclusions

In this work, $LaMnO_3$ soft ferrite nanoparticles were successfully synthesized through the hydrothermal technique and employed as active electrode materials for EDLC-type supercapacitor applications. The fabricated $LaMnO_3$/nickel foam electrodes exhibited excellent electrochemical performance, as confirmed by cyclic voltammetry, galvanostatic charge–discharge, cyclic stability, and electrochemical impedance spectroscopy analyses. The nearly rectangular CV profiles and highly symmetric linear GCD curves confirmed the predominantly non-Faradaic electric double-layer charge storage mechanism of the device. The supercapacitor delivered a maximum specific capacitance of 214 F g^{-1} at a lower current density, which gradually decreased to 75 F g^{-1} at a higher current density due to ion-diffusion limitations and reduced electrolyte accessibility within the porous electrode structure.

'Declaration of Generative AI and AI-assisted technologies in the writing process.'
During the preparation of this manuscript, the authors used Grammarly and AI-assisted technologies for language editing, grammar correction, and improving readability.

Acknowledgment

The authors are grateful to the Department of Physics, Dnyanopasak Shikshan Mandal's Arts, Commerce and Science College, Parbhani, and the School of Physical Sciences, SRTM University, Nanded, for providing laboratory and research facilities to carry out this work. The authors also acknowledge the support of all faculty members and technical staff who assisted during the experimental work.

Financial support and sponsorship

Nil.

Conflicts of interest

The authors declare that there are no conflicts of interest regarding the publication of this paper

References:

1. Ma, Y., Xie, X., Yang, W. *et al.* Recent advances in transition metal oxides with different dimensions as electrodes for high-performance supercapacitors. *Adv Compos Hybrid Mater* **4**, 906–924 (2021). https://doi.org/10.1007/s42114-021-00358-2.
2. Jiang, J., Li, Y., Liu, J., Huang, X., Yuan, C. and Lou, X.W. (2012), Recent Advances in Metal Oxide-based Electrode Architecture Design for Electrochemical Energy Storage. Adv. Mater., 24: 5166-5180. https://doi.org/10.1002/adma.201202146.
3. A. Ray, A. Roy, S. Saha, M. Ghosh, S. R. Chowdhury, T. Maiyalagan, S. K. Bhattacharya, S. Das, Electrochemical Energy Storage Properties of Ni-Mn-Oxide Electrodes for Advance Asymmetric Supercapacitor Application, Langmuir 2019, 35, 25, 8257–8267, https://doi.org/10.1021/acs.langmuir.9b00955.

4. Abbas, Q., Khurshid, H., Yoosuf, R. et al. Engineering of nickel, cobalt oxides and nickel/cobalt binary oxides by electrodeposition and application as binder free electrodes in supercapacitors. Sci Rep 13, 15654 (2023). https://doi.org/10.1038/s41598-023-42647-4.
5. S.L. Kadam, S.M. Mane, P.M. Tirmali, S.B. Kulkarni, Electrochemical synthesis of flower like Mn-Co mixed metal oxides as electrode material for supercapacitor application, Current Applied Physics, 18, 4, 2018, 397-404, https://doi.org/10.1016/j.cap.2018.01.019.
6. Ortega-San-Martin, L. (2020). Introduction to Perovskites: A Historical Perspective. In: Arul, N., Nithya, V. (eds) Revolution of Perovskite. Materials Horizons: From Nature to Nanomaterials. Springer, Singapore. https://doi.org/10.1007/978-981-15-1267-4_1.
7. R. J. H. Voorhoeve, D. W. Johnson, Jr., J. P. Remeika, and P. K. Gallagher, Perovskite Oxides: Materials Science in Catalysis: Perovskite oxides, long known in solid-state chemistry and physics,. find new applications in catalysis. Science, 195, 4281, 827-8331977.
8. Ansari, A.A., Ahmad, N., Alam, M. et al. Physico-chemical properties and catalytic activity of the sol-gel prepared Ce-ion doped LaMnO3 perovskites. Sci Rep 9, 7747 (2019). https://doi.org/10.1038/s41598-019-44118-1.